SUPPORTING INFORMATION

Sarcolipin promotes uncoupling of the SERCA Ca^{2+} pump by inducing a structural rearrangement in the energy-transduction domain

Joseph M. Autry[a,b], David D. Thomas[a], and L. Michel Espinoza-Fonseca[a]*

[a]Department of Biochemistry, Molecular Biology, and Biophysics, [b]Biophysical Technology Center, University of Minnesota, Minneapolis, MN 55455, United States

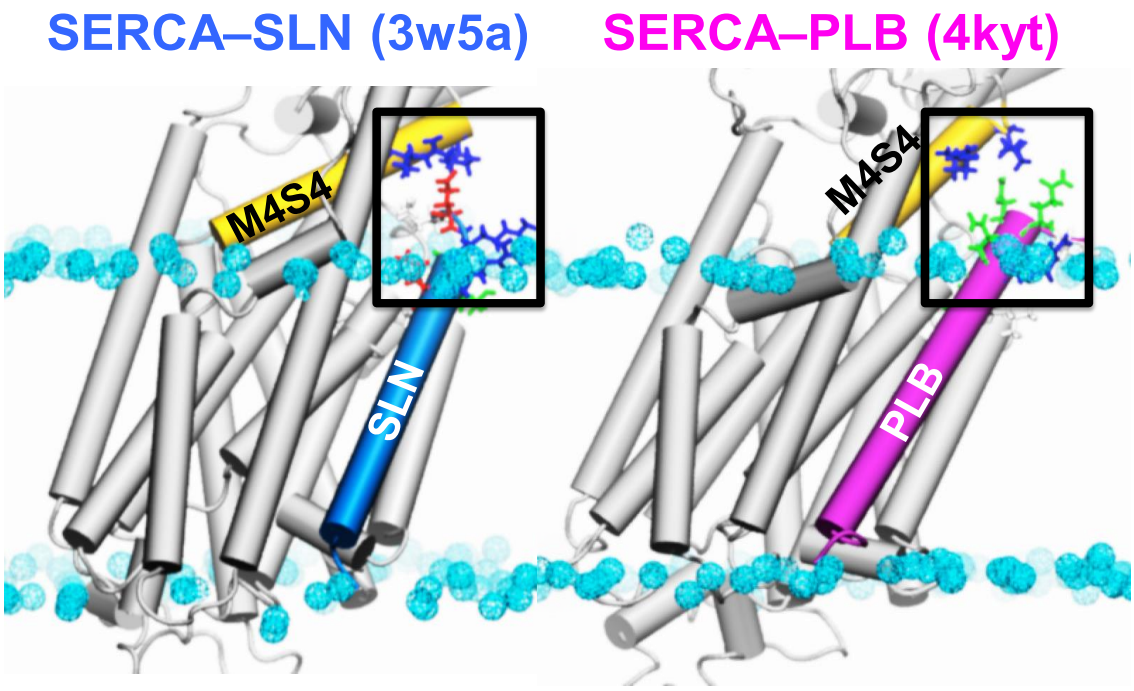

Figure S1. Structural comparison of M4S4 in SERCA–SLN and SERCA–PLB crystal structures. We identified two structural differences between crystal structures of SERCA–SLN[1] and SERCA–PLB[2]. (1) The SERCA–SLN structure (*left panel*) exhibits a bifurcated salt bridge (*black box*) between SLN acidic residue E2 in the cytosolic region and SERCA basic residues K324 and R328 on M4S4 (*yellow cylinder*); these salt bridges do not exist in the SERCA–PLB structure (*right*). (2) The SERCA–SLN structure exhibits a 17° increase in M4S4 tilt angle compared to SERCA–PLB. Proteins are shown in *gray cartoon* representation. Key residues are shown in *stick* colored according to physiochemical property: basic (*blue*), acidic (*red*), and polar (*green*). Phospholipid headgroups of the membrane bilayer are shown as *cyan spheres*.

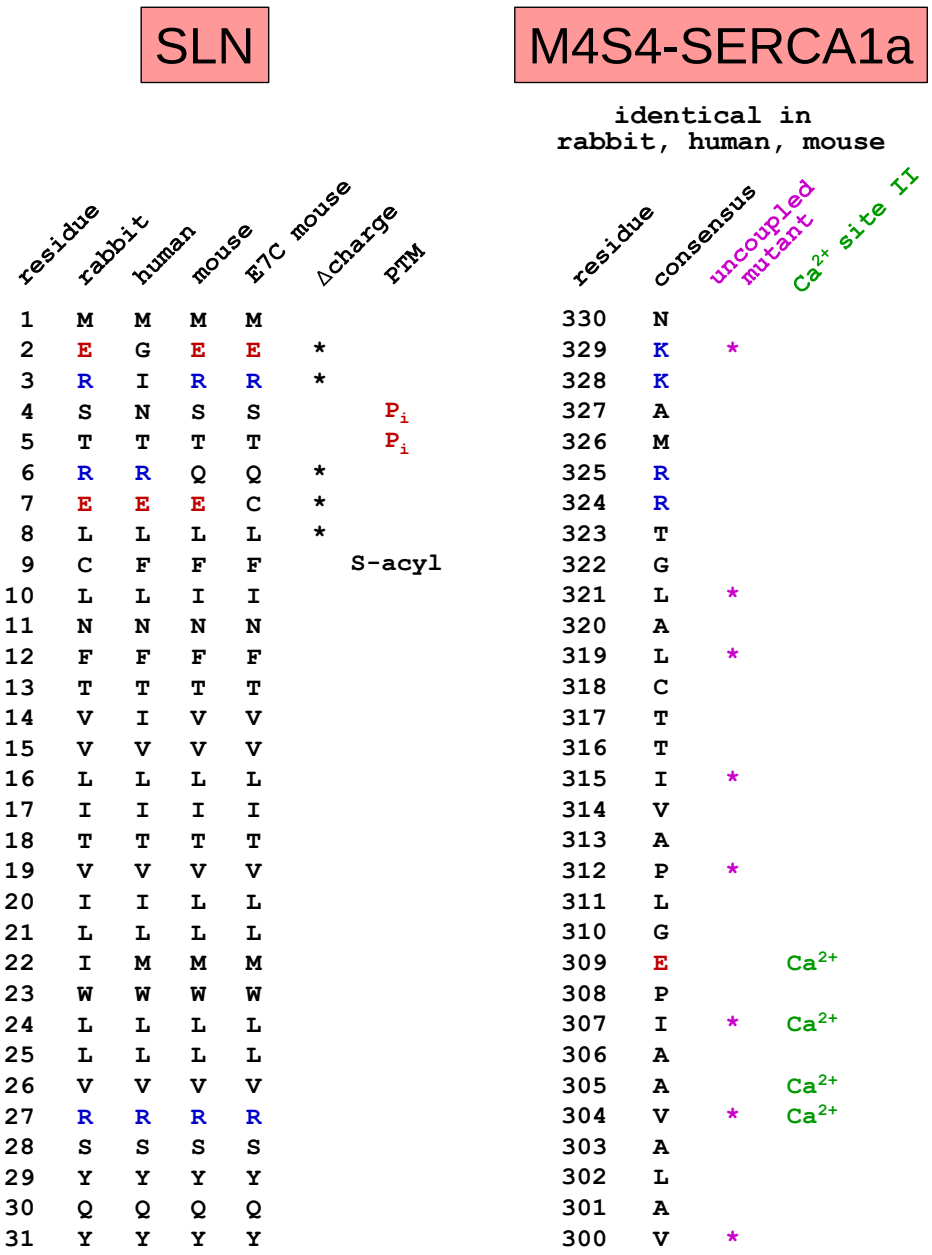

Figure S2. Amino acid sequence alignments of SLN and M4S4 from rabbit, human, and mouse. Residues are color-coded according to physiochemical property: uncharged (*black*), basic (*blue*), and acidic (*red*). LEFT PANEL: Protein sequence alignment of SLN is shown for rabbit,[3] human,[3] mouse[3], and mouse E7C (used for crosslinking[4, 5] and MD simulation[5]). Species sequence variation that results in a change of SLN electrostatic charge is indicated by Δ*charge* (*). Post-translational modifications (*PTM*) of SLN are indicated by *Pi* (phosphorylation of Ser4[6] or Thr5[7]) and *S-acyl* (palmitoylation or oleoylation of Cys9[8]). RIGHT PANEL: Protein sequence alignment for SERCA1a, the Ca^{2+}-ATPase isoform expressed in adult fast-twitch skeletal muscle, is shown for rabbit[9], human[10], and mouse (Genbank AY081946.1). SERCA residues that result in transport/ATPase uncoupling when mutated are indicated by *uncoupled mutant* (*) (for more detail, see **Figure S8**). M4 residues that coordinate the second bound Ca^{2+} ion are indicated by *transport site II* (*Ca^{2+}*): V304 (*backbone carbonyl*), A305 (*backbone carbonyl*), I307 (*backbone carbonyl*), and E309 (*sidechain carboxylate*).[11]

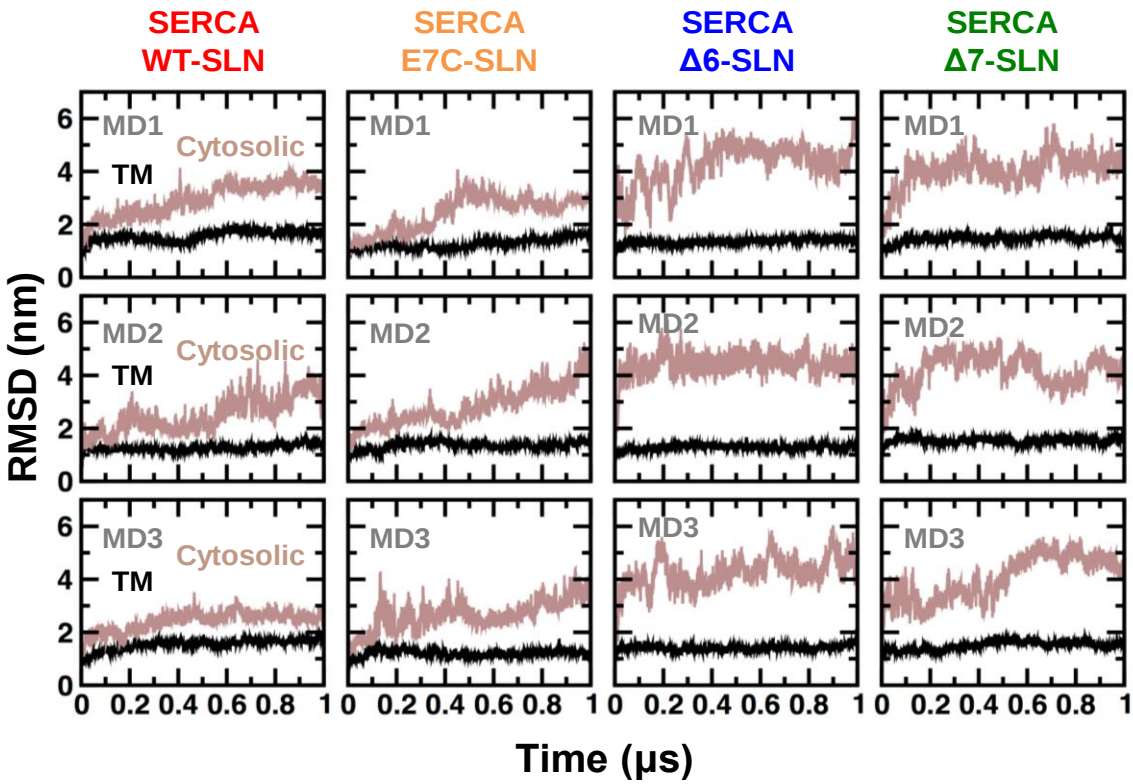

Figure S3. Time-dependent evolution of RMSD for TM and cytosolic domains of SERCA with bound SLN constructs. MDS was performed for SERCA bound to SLN constructs (WT, E7C, Δ6, or Δ7). RMSD was calculated for each independent trajectory relative to the SERCA–SLN crystal structure.[1] RMSD of the TM domain of SERCA (*black*) was calculated using backbone alignment of the ten TM helices (M1–M10). RMSD of the cytosolic headpiece of SERCA (*beige*) was calculated using backbone alignment of the three cytosolic domains (phosphorylation, nucleotide-binding, actuator). The TM domain of SERCA shows low and stable RMSD that is not affected by SLN mutation or truncation, consistent with the stability of SERCA–SLN complexes observed during 1 μs trajectories. The cytosolic headpiece shows moderate and time-dependent RMSD when SERCA is bound with SLN constructs, consistent with MDS studies demonstrating that the SERCA headpiece is inherently dynamic with or without bound SLN or PLB.[12-14]

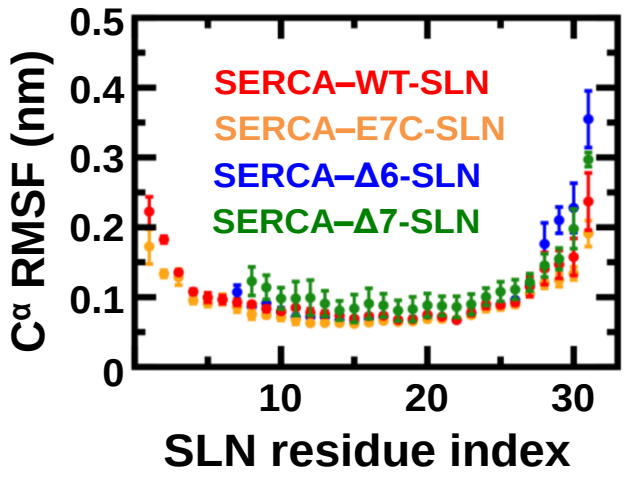

Figure S4. Cα RMSF for SLN constructs bound to SERCA. RMSF is presented as mean ± standard error (*n*=3). MDS indicates that the N-terminus of SLN is moderately rigid for residues 1–3 and more rigid for residues 4–7. Compared to WT-SLN, the E7C-SLN mutant has similar relative mobility for all segments: cytosol (residues 1–8), TM (residues 9–26), and lumen (residues 27–31). Truncation mutants Δ6-SLN and Δ7-SLN maintain rigidity in the TM helix (residues 9–26), yet increase mobility in the luminal C-terminus (residues 27–31), thereby revealing allosteric structural coupling between cytosolic and luminal regions of SLN. Cross-linking[5] and MDS (**Figures 2, 3**) demonstrate that Δ6 truncation of the SLN N-terminus does not cause dissociation of the SERCA–SLN complex. The luminal C-terminus of SLN is involved in inhibition of the Ca^{2+} affinity of SERCA.[15]

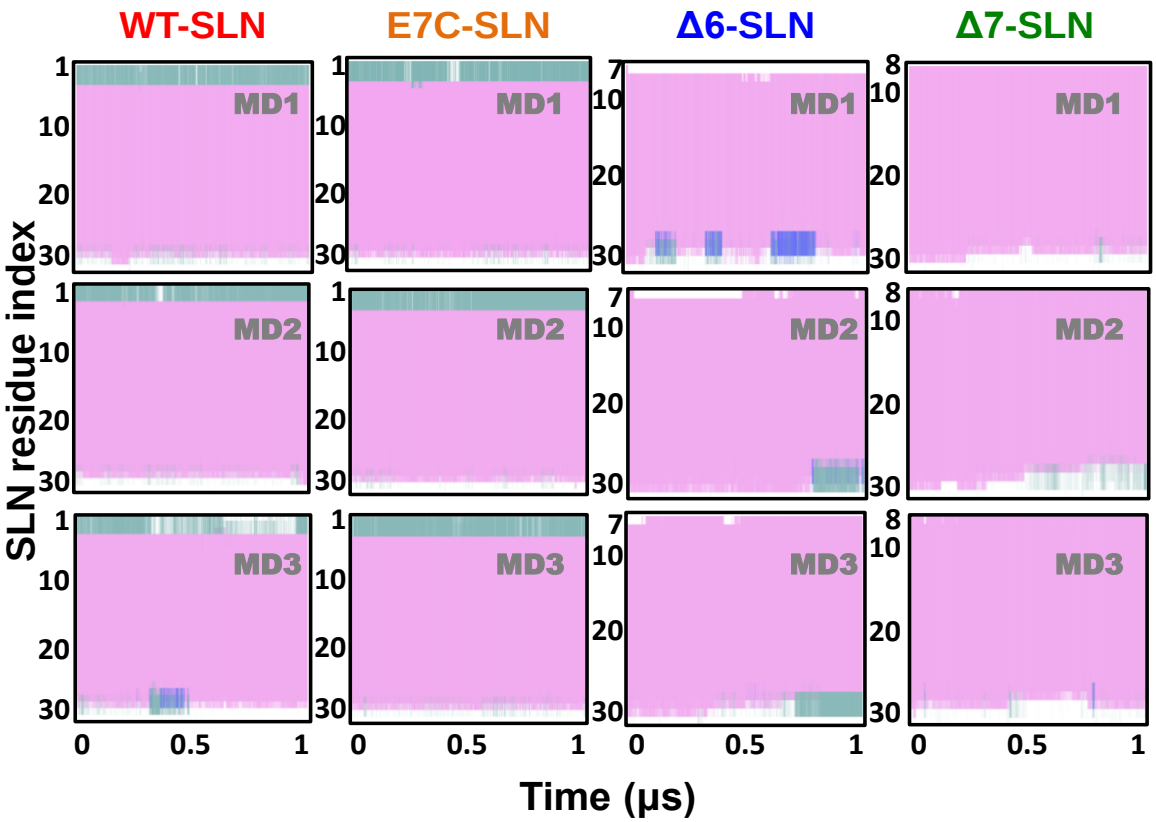

Figure S5. Time-dependent evolution of secondary structure for SLN constructs bound to SERCA. STRIDE[16] was used to analyze the evolution of the secondary structure of SLN in trajectories of SERCA–SLN complexes. Secondary structure is colored with α-helix in *pink*, 3_{10}-helix in *blue*, turn in *cyan*, and coil in *white*. The analysis demonstrates that WT-SLN and E7C-SLN have similar secondary structure in the N-terminus, indicating that the E7C mutation does not alter structural dynamics of the cytosolic region of SLN. The analysis also demonstrates that truncations Δ6 and Δ7 do not alter structural dynamics of the TM domain of SLN (residues 9–26). For Δ6-SLN and Δ7-SLN, the C-terminal tail (residues 27–31) undergoes structural transitions from α-helix to 3_{10}-helix or unfolded on the ns time scale during MDS; this structural interconversion contributes to the small increase in structural fluctuation detected in the C-terminus of Δ6-SLN and Δ7-SLN bound to SERCA (see RMSF in **Figure S4**).

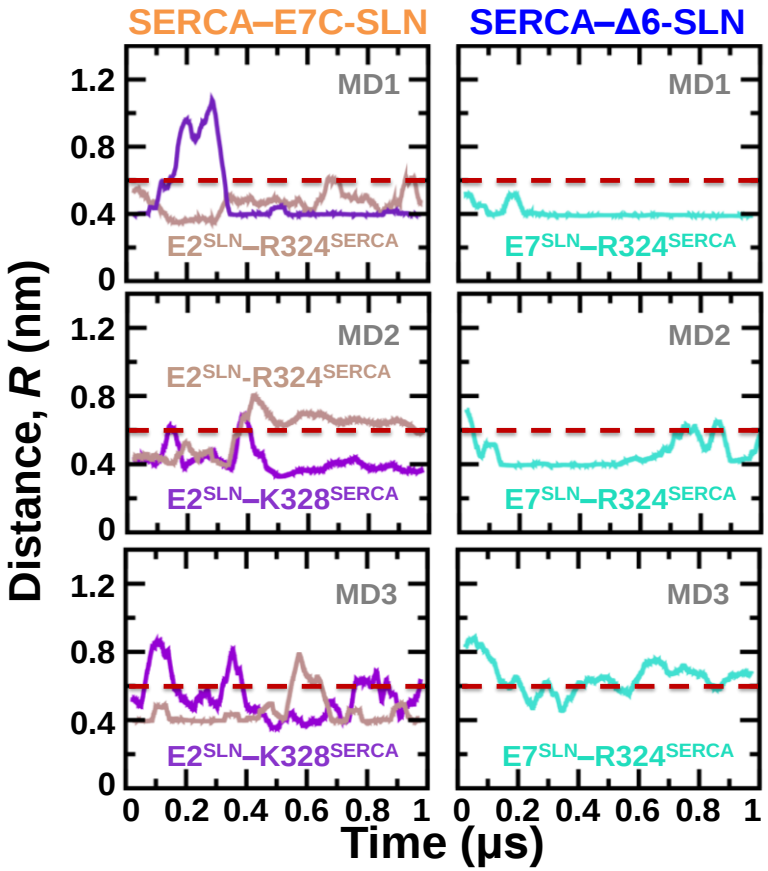

Figure S6. Time-dependent evolution of intermolecular salt bridges between M4S4 and SLN constructs. Distance evolution was calculated between E2^{SLN}–R324^{SERCA} (*beige*) and E2^{SLN}–K328^{SERCA} (*purple*) for E7C-SLN, and between E7^{SLN}–R324^{SERCA} (*cyan*) for Δ6-SLN. The distance (*R*) between E–K and E–R residue pairs was calculated between Cδ–Cζ and Cδ–Nζ atoms, respectively. Inter-residue distance analysis indicates that SLN containing only one glutamate residue at position E2 (i.e., E7C-SLN) forms a bifurcated salt bridge with R324 and K328 on M4S4 of SERCA (*left panel*s; cutoff distance $R \leq 0.6$ nm), similar to the single, bifurcated salt bridge observed in crystal structures among R324 and K328 of M4S4 and E2 of WT-SLN, which contains both E2 and E7 (**Figure 2**). Inter-residue distance analysis indicates that SLN containing only one glutamate residue at position E7 (i.e., Δ6-SLN) forms one intermolecular salt bridge with R324 on M4S4 (*right panel*s; cutoff distance $R \leq 0.6$ nm). These results demonstrate that only one glutamate residue of SLN is needed for salt bridge formation with M4S4 of SERCA, and that multiple salt bridge arrangements are possible.

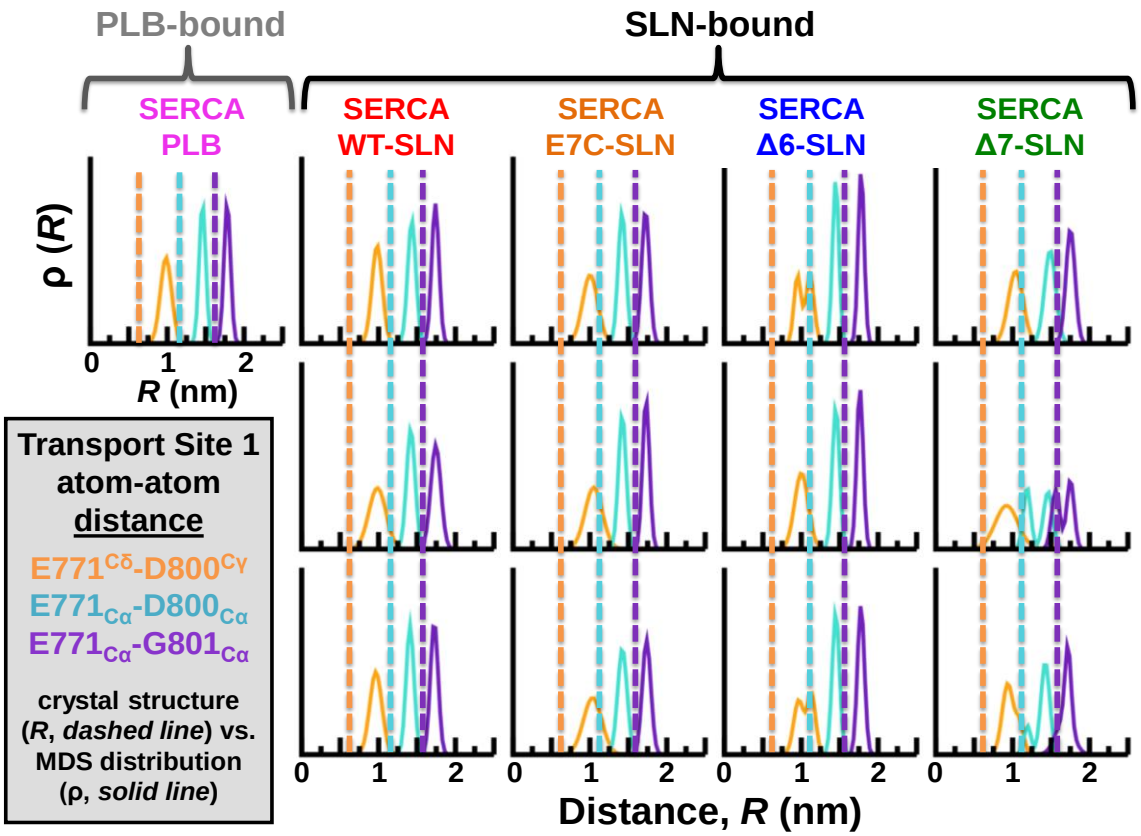

Figure S7. SLN and PLB inhibit the calcium affinity of SERCA by controlling coordination geometry in transport site I. Distance distribution (ρ) between SERCA atom pairs E771$^{C\alpha}$–D800$^{C\alpha}$, E771$^{C\delta}$–D800$^{C\gamma}$, and E771$^{C\alpha}$–G801$^{C\alpha}$ in transport site I were calculated from each 1-μs trajectory for PLB or SLN constructs. The carboxylate side chain of E771 coordinates the Ca^{2+} ion bound in transport site I, while the carboxylate side chain of D800 coordinates the two Ca^{2+} ions bound in transport sites I and II (a bifurcated electrostatic interaction).[11] *Dashed lines* show the atom-atom distance (R) when transport site I adopts a competent, but inhibited, geometry for Ca^{2+} binding, as observed in the crystal structure of SERCA (1su4) grown in 10 mM Ca^{2+}.[11] MDS extends this work to demonstrate that PLB and SLN inhibit SERCA by populating a Ca^{2+}-free intermediate state with inhibited geometry in transport site I, whereby E771 is protonated (i.e., uncharged).[12-14] Here we find that mutation or deletion in the N-terminus of SLN does not reverse structural changes in the transport site I associated with K_{Ca} inhibition,[13, 14] in agreement with experimental data showing that the TM and luminal domains of SLN play the predominant role in lowering the Ca^{2+} affinity of SERCA.[15, 17]

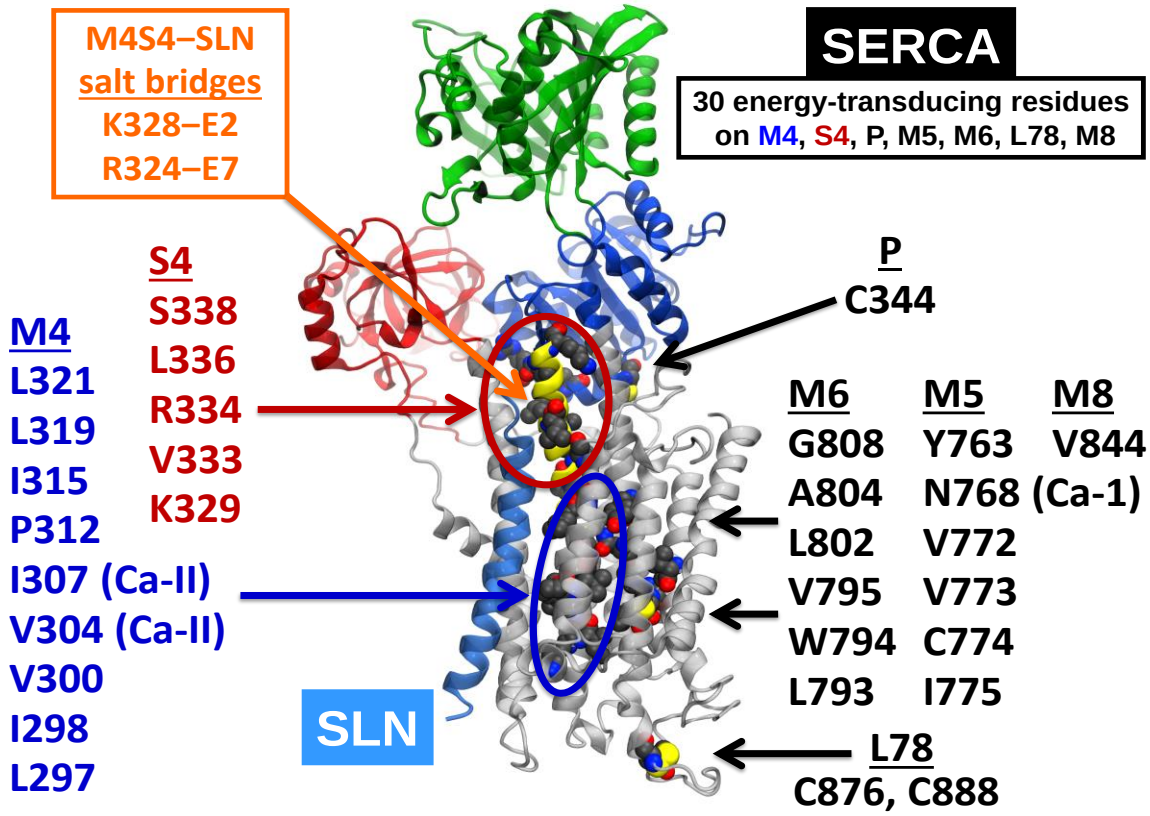

Figure S8. The energy-transduction domain of SERCA is identified by a comprehensive literature search for uncoupled site-directed mutants. A comprehensive review of SERCA literature[18-25] reveals 30 residues which show low Ca^{2+} transport and uncoupled ATPase activity when mutated (single-site substitution). None of these mutants have been reported to show Ca^{2+}-independent ATPase activity. Inesi *et al*. used saturation mutagenesis, dual functional assays at V_{max} condition, and insightful analysis to identify M4S4 as the "energy-transduction segment".[18, 20-22, 26] An illustrative example of functional characterization of an uncoupled mutant is Y763G-SERCA by Andersen *et al*., who show that ATP hydrolysis by the Y763G mutant is Ca^{2+}-dependent, with a WT-like cooperative Ca^{2+} activation of ATP hydrolysis, without concomitant Ca^{2+} transport.[19] Here we define the "energy-transduction domain" as the collection of SERCA residues that are essential for transport/ATPase coupling, and these residues are indicated by topology position: S (*stalk sector*), M (*transmembrane helix*), L (*luminal loop*), and P (*phosphorylation domain*). TM residues that participate in both Ca^{2+} binding and ATPase coupling are indicated for transport site I (*Ca-I*) and transport site II (*Ca-II*). SERCA–SLN salt bridges identified by MDS (**Figure 2**) are listed on the top left (*orange text*). The structural representation of SERCA–SLN was made by Bengt Svensson (U of MN) using PDB code 3w5a.[1]

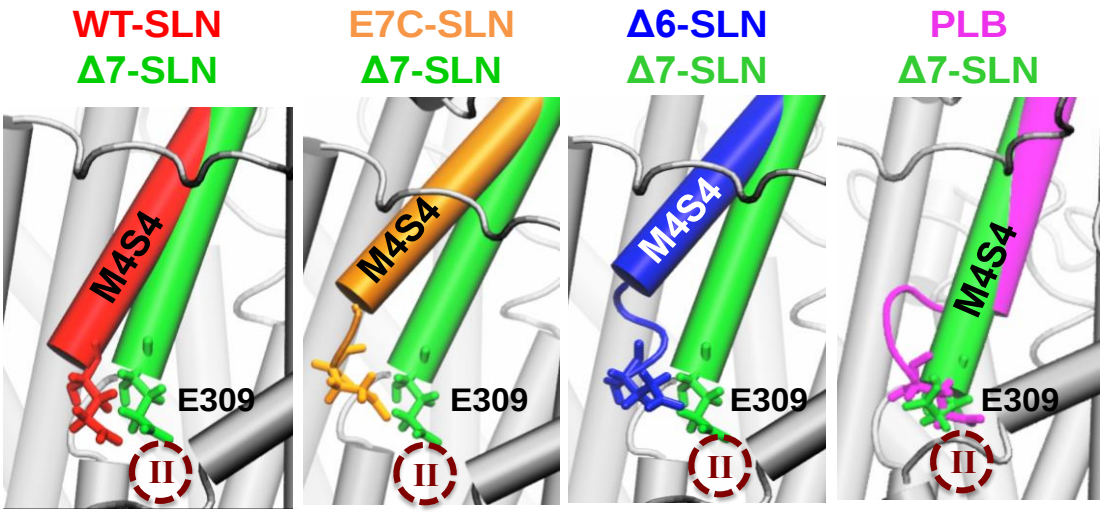

Figure S9. The position of E309 gating residue in transport site II is controlled by M4S4 interaction with SLN, but not PLB. Representative structures extracted from MDS trajectories for WT-SLN (*red*), E7C-SLN (*orange*), Δ6-SLN (*blue*), and PLB (*purple*) are superimposed on a representative MD structure of Δ7-SLN (*green*), a mutant which is unable to decrease the transport efficiency of SERCA. Our MDS results indicate that an increase in M4S4 tilt angle correlates with an increase in the distance of E309 gating residue from transport site II (*dashed circle*); to illustrate, compare the position of E309 in constructs that decrease SERCA coupling ratio (WT-SLN, E7C-SLN, and Δ6-SLN in *left* and *middle panels*)[4, 5] *vs.* constructs that do not affect SERCA coupling ratio (Δ7-SLN and PLB in *right panel*)[4, 5]. We propose that the interaction of SLN–M4S4 produces a unique structural rearrangement of the E309 gating residue[27, 28] that perturbs Ca^{2+} occlusion in transport site II and thus facilitates Ca^{2+} slippage back to the cytosol.

SI METHODS

Setting up SERCA–SLN complexes for simulation

We used the crystal structure of E1•Mg^{2+}-SLN (PDB code 3w5a[1]) as a starting structure for MDS. We modeled four SLN constructs bound to SERCA: WT-SLN, E7C-SLN, Δ6-SLN, and Δ7-SLN. On the basis of our previous MDS studies,[13, 14] we simulated the four SERCA–SLN systems at appropriate physiological conditions by removing Mg^{2+} from the transport sites and by modeling transport site residues E309 and D800 as unprotonated (i.e., ionized), and residues E771 and E908 as protonated (i.e., uncharged). Protonation of transport site residues E771 and E908 was verified using PROPKA version 3.1,[29, 30] a program that estimates empirical pK_a values of ionizable groups in proteins and protein-protein complexes based on the 3D structure, plus explicit incorporation of Coulombic interactions that arise from mutually titrating residues via the Tanford-Roxby procedure.[31] SERCA–SLN complexes were inserted in a 12×12 nm bilayer of POPC (1-palmitoyl-2-oleoyl-sn-glycero-3-phosphocholine) and solvated using TIP3P water molecules. K^+ and Cl^- ions were added to produce concentrations of 100 mM and 110 mM, respectively. CHARMM36 force field topologies and parameters were used for proteins,[32] POPC,[33] water, K^+, and Cl^-.

Setting up the SERCA–PLB complex for simulation

We used an atomic model of WT-PLB bound to SERCA generated in our recent study to simulate the inhibited SERCA–PLB complex.[14] On the basis of this study, we modeled transport site residues E309 and D800 as unprotonated (ionized) and residues E771 and E908 as protonated (uncharged). Protonation of transport site residues E771 and E908 was verified using PROPKA 3.1.[29, 30] The SERCA–PLB complex was inserted in a 12×12 nm bilayer of POPC and solvated using TIP3P water molecules. K^+ and Cl^- ions were added to produce concentrations of 100 mM and 110 mM, respectively. CHARMM36 force field topologies and parameters were used for proteins,[32] POPC,[33] water, K^+, and Cl^-.

Molecular dynamics simulation

MDS of SERCA–SLN constructs and SERCA–PLB was performed using the program NAMD version 2.11[34] with periodic boundary conditions,[35] particle mesh Ewald,[36, 37] a non-bonded cutoff of 0.9 nm, and a 2 fs time step. The NPT ensemble was maintained with a Langevin thermostat (310 K) and an anisotropic Langevin piston barostat (1 atm). Fully-solvated systems were first subjected to energy minimization, followed by gradually warming up of the systems for 200 ps. This procedure was followed by 10 ns of equilibration with backbone atoms harmonically restrained using a force constant of 1000 kcal mol^{-1} nm^{-2}. We performed 13 independent 1-μs MD simulations: 3 independent runs with initial random velocities for each SERCA–SLN construct, and one run for SERCA–PLB.

Structure analysis and visualization

The VMD program[38] was used for analysis, visualization, and rendering of structures. The STRIDE program[39] was used to analyze secondary structure evolution of SLN constructs bound to SERCA. STRIDE recognizes secondary structural elements in proteins from their atomic coordinates, and it utilizes both hydrogen-bond energy and main chain dihedral angles to define the secondary structure pattern, relying on database-derived recognition parameters with crystallographic definitions of secondary structure as the standard-of-truth.[39]

SI REFERENCES

(1) Toyoshima, C., Iwasawa, S., Ogawa, H., Hirata, A., Tsueda, J., and Inesi, G. (2013) *Nature 495*, 260-264.
(2) Akin, B. L., Hurley, T. D., Chen, Z., and Jones, L. R. (2013) *J Biol Chem 288*, 30181-30191.
(3) Odermatt, A., Taschner, P. E., Scherer, S. W., Beatty, B., Khanna, V. K., Cornblath, D. R., Chaudhry, V., Yee, W. C., Schrank, B., Karpati, G., Breuning, M. H., Knoers, N., and MacLennan, D. H. (1997) *Genomics 45*, 541-553.
(4) Sahoo, S. K., Shaikh, S. A., Sopariwala, D. H., Bal, N. C., and Periasamy, M. (2013) *J Biol Chem 288*, 6881-6889.
(5) Sahoo, S. K., Shaikh, S. A., Sopariwala, D. H., Bal, N. C., Bruhn, D. S., Kopec, W., Khandelia, H., and Periasamy, M. (2015) *J Biol Chem 290*, 14057-14067.
(6) Gramolini, A. O., Trivieri, M. G., Oudit, G. Y., Kislinger, T., Li, W., Patel, M. M., Emili, A., Kranias, E. G., Backx, P. H., and MacLennan, D. H. (2006) *Proc Natl Acad Sci U S A 103*, 2446-2451.
(7) Bhupathy, P., Babu, G. J., Ito, M., and Periasamy, M. (2009) *J Mol Cell Cardiol 47*, 723-729.
(8) Montigny, C., Decottignies, P., Le Marechal, P., Capy, P., Bublitz, M., Olesen, C., Møller, J. V., Nissen, P., and le Maire, M. (2014) *J Biol Chem 289*, 33850-33861.
(9) Brandl, C. J., deLeon, S., Martin, D. R., and MacLennan, D. H. (1987) *J Biol Chem 262*, 3768-3774.
(10) Zhang, Y., Fujii, J., Phillips, M. S., Chen, H. S., Karpati, G., Yee, W. C., Schrank, B., Cornblath, D. R., Boylan, K. B., and MacLennan, D. H. (1995) *Genomics 30*, 415-424.
(11) Toyoshima, C., Nakasako, M., Nomura, H., and Ogawa, H. (2000) *Nature 405*, 647-655.
(12) Espinoza-Fonseca, L. M., Autry, J. M., and Thomas, D. D. (2014) *PLoS One 9*.
(13) Espinoza-Fonseca, L. M., Autry, J. M., and Thomas, D. D. (2015) *Biochem Biophys Res Commun 463*, 37-41.
(14) Espinoza-Fonseca, L. M., Autry, J. M., Ramirez-Salinas, G. L., and Thomas, D. D. (2015) *Biophys J 108*, 1697-1708.
(15) Gorski, P. A., Glaves, J. P., Vangheluwe, P., and Young, H. S. (2013) *J Biol Chem 288*, 8456-8467.
(16) Frishman, D., and Argos, P. (1995) *Proteins 23*, 566-579.
(17) Asahi, M., Sugita, Y., Kurzydlowski, K., De Leon, S., Tada, M., Toyoshima, C., and MacLennan, D. H. (2003) *Proc Natl Acad Sci U S A 100*, 5040-5045.
(18) Zhang, Z., Sumbilla, C., Lewis, D., and Inesi, G. (1993) *FEBS Lett 335*, 261-264.
(19) Andersen, J. P. (1995) *J Biol Chem 270*, 908-914.
(20) Zhang, Z., Sumbilla, C., Lewis, D., Summers, S., Klein, M. G., and Inesi, G. (1995) *J Biol Chem 270*, 16283-16290.
(21) Chen, L., Sumbilla, C., Lewis, D., Zhong, L., Strock, C., Kirtley, M. E., and Inesi, G. (1996) *J Biol Chem 271*, 10745-10752.
(22) Garnett, C., Sumbilla, C., Belda, F. F., Chen, L., and Inesi, G. (1996) *Biochemistry 35*, 11019-11025.
(23) Daiho, T., Yamasaki, K., Saino, T., Kamidochi, M., Satoh, K., Iizuka, H., and Suzuki, H. (2001) *J Biol Chem 276*, 32771-32778.
(24) Miyauchi, Y., Daiho, T., Yamasaki, K., Takahashi, H., Ishida-Yamamoto, A., Danko, S., Suzuki, H., and Iizuka, H. (2006) *J Biol Chem 281*, 22882-22895.
(25) Xu, C., Prasad, A. M., Inesi, G., and Toyoshima, C. (2008) *J Biol Chem 283*, 3297-3304.
(26) Zhang, Z., Lewis, D., Strock, C., Inesi, G., Nakasako, M., Nomura, H., and Toyoshima, C. (2000) *Biochemistry 39*, 8758-8767.
(27) Inesi, G., Ma, H., Lewis, D., and Xu, C. (2004) *J Biol Chem 279*, 31629-31637.
(28) Clausen, J. D., Bublitz, M., Arnou, B., Montigny, C., Jaxel, C., Møller, J. V., Nissen, P., Andersen, J. P., and le Maire, M. (2013) *EMBO J 32*, 3231-3243.
(29) Olsson, M. H. M., Sondergaard, C. R., Rostkowski, M., and Jensen, J. H. (2011) *J Chem Theory Comput 7*, 525-537.
(30) Sondergaard, C. R., Olsson, M. H. M., Rostkowski, M., and Jensen, J. H. (2011) *J Chem Theory Comput 7*, 2284-2295.
(31) Tanford, C., and Roxby, R. (1972) *Biochemistry 11*, 2192–2198.
(32) Best, R. B., Zhu, X., Shim, J., Lopes, P. E., Mittal, J., Feig, M., and Mackerell, A. D., Jr. (2012) *J Chem Theory Comput 8*, 3257-3273.
(33) Klauda, J. B., Venable, R. M., Freites, J. A., O'Connor, J. W., Tobias, D. J., Mondragon-Ramirez, C., Vorobyov, I., MacKerell, A. D., Jr., and Pastor, R. W. (2010) *J Phys Chem B 114*, 7830-7843.
(34) Phillips, J. C., Braun, R., Wang, W., Gumbart, J., Tajkhorshid, E., Villa, E., Chipot, C., Skeel, R. D., Kale, L., and Schulten, K. (2005) *J Comput Chem 26*, 1781-1802.
(35) Weber, W., Hünenberger, P. H., and McCammon, J. A. (2000) *J Phys Chem B 104*, 3668-3675.
(36) Darden, T., York, D., and Pedersen, L. (1993) *J Chem Phys 98*, 10089-10092.
(37) Essmann, U., Perera, L., and Berkowitz, M. L. (1995) *J Chem Phys 103*, 8577-8593.
(38) Humphrey, W., Dalke, A., and Schulten, K. (1996) *J Mol Graph 14*, 33-38, 27-38.
(39) Frishman, D., and Argos, P. (1995) *Proteins: Struc Func and Genet 23*, 566-579.